NP-12651

SUMMARY OF SHERWOOD ACTIVITIES SUPPLEMENTARY REPORT

15 FEBRUARY 1963

HEADQUARTERS FIELD COMMAND
DEFENSE ATOMIC SUPPORT AGENCY
SANDIA BASE, ALBUQUERQUE, NEW MEXICO

(5) 782600

HEADQUARTERS FIELD COMMAND
DEFENSE ATOMIC SUPPORT AGENCY
SANDIA BASE, ALBUQUERQUE, NEW MEXICO

(7) NA
(8) NA
(10) 37 p. incl. illus. tables

(6) SUMMARY OF SHERWOOD ACTIVITIES

SUPPLEMENTARY REPORT

(11) (Rept. no. NP-12651, Suppl. to Rept. no. NP-12171, AD-291159)

(12) NA

(13) NA

(9) 15 Feb[redacted]63

fd

AD-291 159

FOREWORD

This report supplements the report "Summary of SHERWOOD Activities," dated 15 August 1962 and contains current information relating to research, fabrication and experimentation in controlled thermonuclear reactions. The Supplement therefore should be used in conjunction with the 15 August 1962 publication.

The Supplement updates research in progress and experimental devices used at the four Atomic Energy Commission laboratories principally involved in SHERWOOD and at various other research facilities. Material included has been obtained primarily from laboratory publications and from visits to the experimental facilities. The report has not been reviewed by the laboratories.

A new complete summary is scheduled for publication in August 1963.

This supplemental report was prepared by the members of the Research Division, Field Command, Defense Atomic Support Agency.

FOR THE COMMANDER:

Louis W. Pflanz, Jr.

LOUIS W. PFLANZ, JR.
Colonel USA
Director, Research Division

TABLE OF CONTENTS

		PAGE NR
Foreword		ii
List of Illustrations		iv
III.	Experimental Devices and Research at the Los Alamos Scientific Laboratory	1
IV.	Experimental Devices and Research at the Lawrence Radiation Laboratory	11
V.	Experimental Devices and Research At Oak Ridge National Laboratory	17
VI.	Experimental Devices and Research at Princeton University	25
VII.	Other Experimental Devices and Research in the United States:	30
	Massachusetts Institute of Technology, Cambridge, Mass. Naval Research Laboratory, Washington, D. C. Stevens Institute of Technology, Hoboken, New Jersey	
VIII.	Experimental Devices and Research in Foreign Nations:	35
	Federal Republic of Germany United Kingdom France	
Distribution		36

LIST OF ILLUSTRATIONS

FIGURE	TITLE	PAGE NR.
1-S.	Diagram of Coaxial Fast Linear Pinch Plasma Gun	2
2-S.	SCYLLA IV Coil With Schematic Circuit Added	4
3-S.	SCYLLA I External Probe Measurement Experiment	6
4-S.	Large Bore Hydromagnetic Gun	8
5-S.	Coaxial Plasma Gun for Injection into a Mirror Field	10
6-S.	Schematic Diagram of HOMOPOLAR V Device	14
7-S.	Schematic Diagram of Modified HOTHOUSE Apparatus	16
8-S.	Slow Ion Plasma Drift in DCX-1	18
9-S.	A Schematic Drawing of the Electron Cyclotron Heating Experiments	20
10-S.	Schematic Blanket Design for a Thermonuclear Reactor	22
11-S.	Sketch of Electron-Beam Plasma Injection Apparatus	24
12-S.	Plasma Injection Experiment	29
13-S.	Electron-Beam-Plasma Interaction Experiment	31

SECTION III

EXPERIMENTAL DEVICES AND RESEARCH AT THE LOS ALAMOS SCIENTIFIC LABORATORY

NOTE: The major sections of this supplementary report are arranged in the same sequence used in the 15 August 1962 report, with the numbering of the major sections corresponding to the numbering used therein. In cases where no new information is available, the section and the number are omitted. To differentiate between diagram numbers used in the 15 August Summary and in this Supplement, the suffix S is used herein.

3-2.5 FAST COAXIAL GUN EXPERIMENT. The experimental arrangement is shown in Figure 1-S. The geometry and parameters are similar to those of FILIPE except that no attempt was made to pinch the gun plasma output. The gun generated plasma was diagnosed with (1) B field momentum analyzer employing a Faraday cup to collect axial component ions, (2) a D_2O ice target to measure transverse component ions, and (3) magnetic probes to measure ions along the gun barrel.

3-2.5.1 OPERATION. Operation was performed in the high pressure and low pressure modes. The high pressure mode is characterized by the admittance of large amounts of D_2 gas through the inner electrode ports before capacitor discharge resulting in a low energy plasma. The low pressure mode is characterized by the admittance of small amounts of gas through the ports resulting in high energy ions - up to 270 Kev (average ~ 240 Kev). The mechanism by which ions are accelerated to energies about ten times the applied voltage is not fully understood. Results described below apply to the low pressure, high energy mode.

3-2.5.2 RESULTS. Two groups of deuterons are observed during each discharge. One group ($\sim 10^{11}$ total ions) is emitted from a central region immediately in front of the center electrode and is measured by projecting the beam through defining slits into an ion deflecting magnetic field. The energy spread is between 12 and 270 Kev. Particle density of these axial deuterons is $\sim 10^8$ ions cm^{-3}. Momentum measurements indicated that slow ions arriving at the analyzer ahead of the fast ions must be born some 30 cm down the tube with the fast ions being created at the face of the inner electrode. The other group of deuterons consisting of about 10^{16} ions per burst lie in the 100 Kev range. This group diverges into the walls of the drift chamber. The high resolution cross-section of deuterium ice (D_2O) was utilized to show that the nominal shape is a diverging hollow cone of ions. The divergence can be reduced by an axial magnetic field and influenced by a longer outer electrode. The bulk of the fast ions appear to follow a curved trajectory from the muzzle into the drift tube. The curvature can be explained by a space charge expansion of the beam or by bending of the ions in the B field of a current (~300 A) flowing along the center electrode. Particle density is $\sim 10^{10}/cm^3$.

3-2.5.3 THE ACCELERATION MECHANISM. It is believed that the high energy particles result from a rapid current drop which builds up the E field component. E x B forces then accelerate the ions to very high velocities. As the discharge begins, current begins to flow along the outer surfaces of the gas. As ionization proceeds, current builds up and is accompanied by a magnetic field which tends to impede the flow of ions (pinch mechanism). This process continues until all the gas is ionized at which time the flow of ions is suddenly pinched off and the current drops sharply and causes a build up of the electric field. This instability

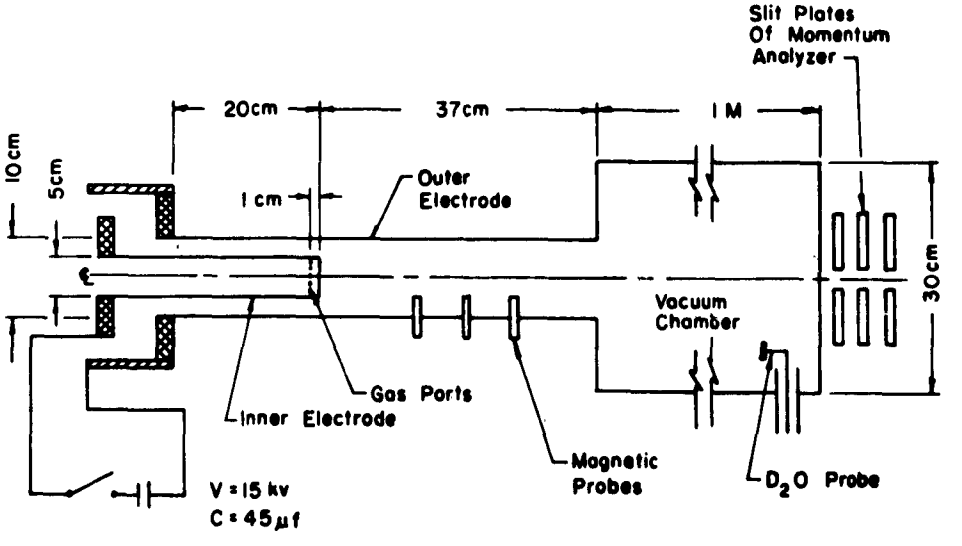

Figure 1-S. Diagram of Coaxial Fast Linear Pinch Plasma Gun

pinch occurs when only ~10 percent of available capacitor energy has been used. Efforts to use larger quantities of gas result in a faster current breakdown which perhaps explains the lower energy particles produced in the high pressure mode.

3-2.5.4 PLANS. Planned experimentation indicates (1) a study of plasma behavior using a longer inner electrode, (2) extensive magnetic probe measurements, (3) use of a D_2O detector along the surface of the inner electrode to determine neutron distribution, and (4) use of a camera to photograph the discharge.

3-4.4 SCYLLA III PREIONIZER. The preionizer installed on SCYLLA III was put into operation and produced a clean plasma with deuteron ion energies up to 800 ev (previous energy 500 ev). It was determined that electron energies are not a function of the trapped magnetic field strength.

3-4.5 SCYLLA IV. Construction of this device (Figure 2-S) is complete; it is designed to confine hot (5 Kev), dense (10^{18} cm^{-3}) plasma for 50 μsec in magnetic fields up to 250 K gauss. Initial experimentation will be conducted with a mirror ratio of 1. The circuit consists of four banks of capacitors; the preionizer bank (PI), the primary bank (PB), the bias field bank (B_O), and the secondary bank (SB; ZEUS Bank). Energy delivered to the coil will be ~3.5 megajoules. A massive coil clamp (2 tons) was installed over the coil and collector plate taper sections to hold this portion of the device together. The collector plates are 15 feet long, 15 feet wide, 3 inches thick and are held together by 140, 4000 pound tensile strength bolts.

3-4.5.1 OPERATIONAL CONCEPT. The slow B_O field will be applied; ionization is achieved before application of the PB and SB banks by superimposing the sharp, short duration PI bank discharge on the B_O field. Applying the fast PI bank reverses the magnetic field and initiates the theta pinch. The process is completed when the large slow ZEUS bank is discharged into the coil. A difficulty presently being experienced is in the perfection of a switch which will accept the SB bank after discharge of the PB bank.

3-4.5.2 OPERATION. The preionizer and B_O banks are in operation. Emphasis is placed on the production of a clean plasma by the PI bank. As a result, impurities and electron temperature are being studied as functions of (1) pressure of the deuterium, (2) energy storage of the PI bank, and (3) the B_O field. Diagnostics include the use of a monochromator to look at the Balmer series edge near the continuum and a spectrograph which can look at impurities down to λ 200 A.

3-4.5.3 PLANS. The primary bank is expected to be in operation by March 1963. Interest then will be in stability of the plasma in the coil; e.g., has the increased length of the coil increased the stability? Experiments already performed on SCYLLA III probably will be repeated on SCYLLA IV.

3-5.5 RESULTS OF ZEEMAN EXPERIMENT. Measurements were made by applying a direct current and using the Neon line at ~λ 2200 Å and the Carbon III (C-III) at λ 2296 Å. The C-III line served as cold (17-18 ev) calibration line during the first half-cycle of the driving magnetic field. The C-V (λ 2271 Å) line appears (ionization at ~300 ev) just before peak compression and disappears as the plasma temperature rises in the second half-cycle. The C-V data obtained during second half-cycle was scaled to the first-half cycle C-III data (B field known) at a time when the external and plasma fields are equal. Hence the B field can be measured utilizing the ZEEMAN effect. Results indicate that a 0 to 10 K gauss field exists in the fireball before peak

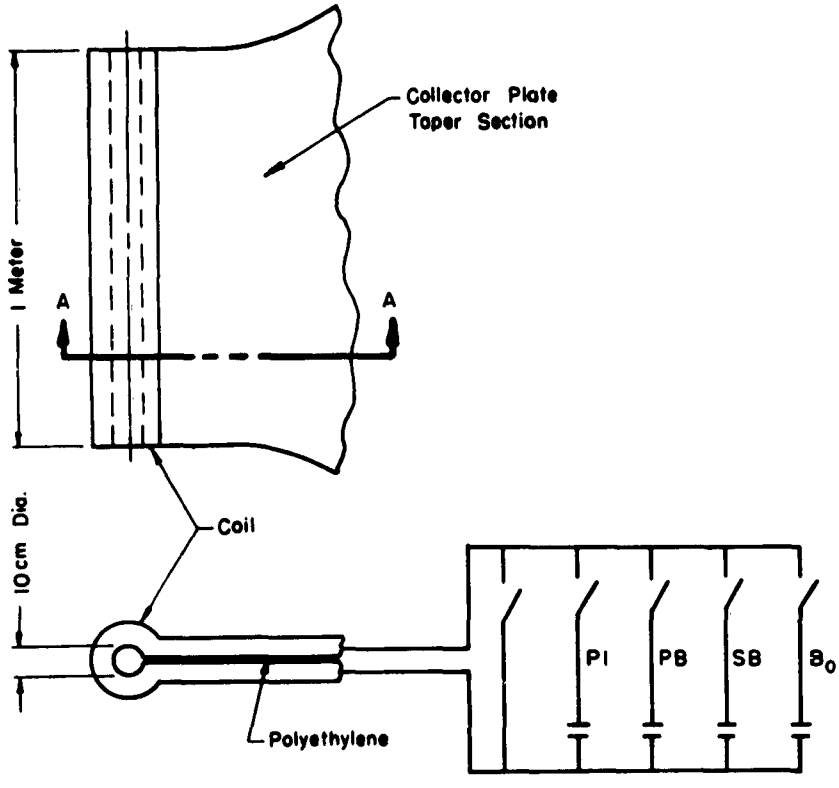

SECTION A-A With Schematic Circuit Added

Bank	Capacity (μf)	Potential (Kv)	Energy (Kj)	τ/4 (μs)	B (K gauss)
PI	12	40	9.6	0.9	11
B_O	5,600	10	280.0	52.0	12
PB	432	50	540.0	3.6	110
SB	15,000	20	3,000.0	25.0	250

Figure 2-S. SCYLLA IV Coil With Schematic Circuit Added

compression. The lower limit for β is 0.9. Work is continuing with the B-IV and O-V lines (near λ 2800 Å) to verify the results obtained using the C-V line.

3-5.5.1 EXTERNAL PROBE MEASUREMENT. A small external magnetic probe placed inside the coil, but outside the ceramic discharge tube, has been used to measure the magnetic field inside the SCYLLA I plasma, Figure 3-S.

3-5.5.1.1 MEASUREMENT TECHNIQUE. When a diamagnetic plasma exists, lines of magnetic field excluded from the plasma are compressed into the space between the plasma and the conducting coil, increasing the flux threading the external coil compared to that in the vacuum by approximately the inverse ratio of the areas available to the flux inside and outside the vacuum. The probe is connected in series with a compensating loop which detects the magnetic field outside the SCYLLA I coil and is adjusted so that the rate of flux change is equal and opposite in the absence of a plasma. When a plasma is present the net difference signal (Δ) is measured.

3-5.5.1.2 RESULTS. The external magnetic field rises to 55 K gauss in 1.25 μ sec and produces a hot deuterium plasma with a density of $5 \times 10^{16}/cm^3$ which emits neutrons and soft x-rays for about 0.8 μ sec at the maximum of the second half-cycle of the driving magnetic field. Previous measurements with probes immersed in the fireball show that the magnetic field is excluded from the plasma (diamagnetic; $\beta = 1$) early in the first half-cycleand that it breaks into the plasma near its peak. It was believed that cold impurities from the immersed probe cooled the plasma and caused the external field breakthrough. The external field probe technique which does not perturb the plasma shows definitely that the magnetic field br akthrough occurs because of the presence of the immersed probe.

3-5.5.2 SCYLLA I X-RAY EXPERIMENTS. X-ray work is continuing with a potassium acid phthalate (KAP) crystal Bragg spectrometer for studying x-rays in the 15 to 25 Å region. Measurements of the continuum spectrum were unsuccessful. Measurement of the second crystal lattice spacing of KAP at ~26 Å (compared to previous crystal spacing of ~ 16 Å) extended spectrum measurements to include the entire O-VIII Lyman Series as well as the O-VII. Good Doppler broadening data were obtained for the C-V line and previously collected Ne-IX line data have been rechecked and found to confirm the results. Since line broadening is expected to be due entirely to Doppler effect, the line width can be reduced to an apparent ion temperature. ($\beta = 1 = 3nkT\,(8\pi)/B^2$), in this case 9.3 ± 2.8 Kev for both O-VII and O-VIII ions. This temperature is much higher than the apparent deuteron temperature of 1.3 Kev, and it is necessary to invoke some non-thermal process to explain it, e.g., a microturbulence driving all ions to the same velocity ($\sim 3 \times 10^7$ cm/sec) in which case $T_i \propto M_i$, or acceleration of ions by local E fields ($T_i \propto Z^2/M_i$). The accuracy of the measurements is not quite good enough to determine the mechanism, although when the C-V line at λ 2271 Å is included, an M_i dependence of T_i is suggested.

3-7.2 PICKET FENCE III. Emphasis is being placed on understanding individual particle behavior in this entropy trapping experiment conducted in a cusped field geometry. An electrostatic ion energy analyzer has been used to measure the flux of ions leaving the B field for various ion energies, e.g., 9 Kev to 20 Kev for deuterons. The flux varies approximately as t^{-k} ($10\,\mu$ sec $< t <$ 1 msec), where k lies between 1.5 and 2.5. The value of k increases with base vacuum pressure before injection but is not strongly dependent on ion energy. Since

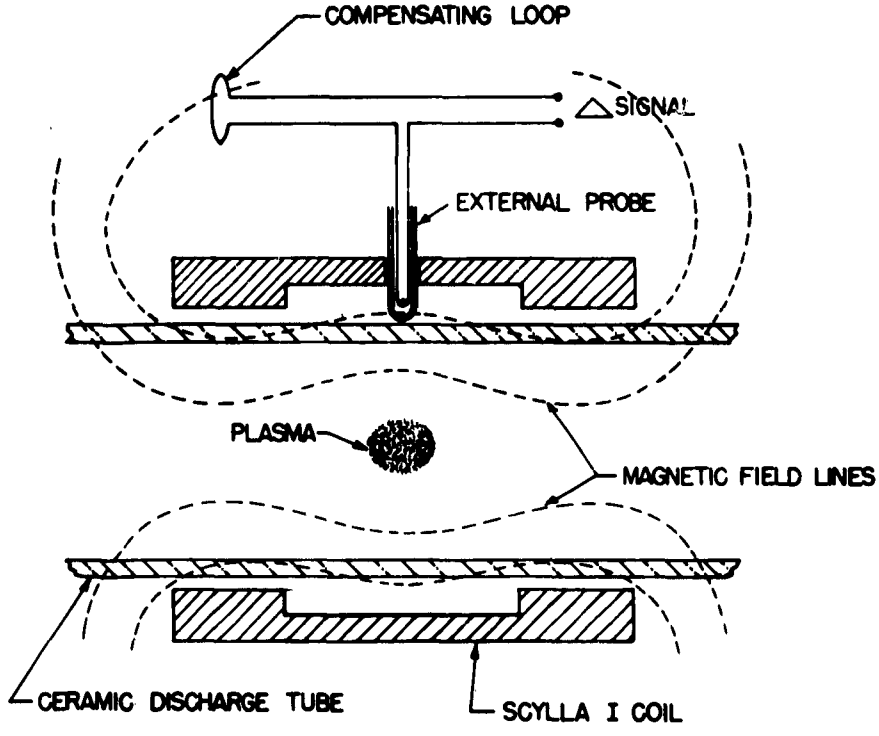

Figure 3-S. SCYLLA I External Probe Measurement Experiment

the flux is a measure of the ion loss rate, the number confined as a function of time may be obtained by integration; i.e., $N \propto t^{-k}$ $(0.5 < k < 1.5)$. This result suggests a binary-diffusion loss process for which $N \propto t^{-1}$. The M/Z ratio for 14 Kev ions was found to be 2. This result was obtained at 250 μ sec after injection by simultaneous measurements of $(M/Z)\ V^2$ in the electrostatic energy analyzer and of V in an E x B drift space. This value of 2 does not rule out the presence of very energetic heavy ions, e.g., O-IX, instead of deuteron; however, this probability seems unlikely from energy considerations.

3-7.2.1 PLANS. Since ion loss has been observed at off-axis points and in directions not parallel to the field lines, use will be made of several detectors to obtain simultaneously an overall picture of ion and electron loss.

3-8.4 PICKET FENCE II B. To alleviate the erratic production of neutrons and x-rays and permit operation at higher injected gas pressures, the energy source was changed from a 6μf, 25 Kv capacitor bank to an ignitron-switched 16μf, 20 Kv bank. This change raised available energy from 1800 to 3000 joules.

3-8.4.1 X-RAY EXPERIMENTS. Studies were made with the new bank to determine the effect of electrode materials and capacitor bank parameters on the x-ray signal. Electrode surfaces of Ta, stainless steel, Al, and brass were found to increase the average x-ray yield respectively; brass produced approximately 10 times the average yield for Ta. Absorption curves for a counter located near the exit cusp show, in general, a distinct soft x-ray component with an average x-ray energy, E, for the brass electrode which varies with the magnetic field as follows: $E \simeq 195$ Kev for B = 5.4 K gauss, $E \simeq 175$ Kev for B = 3.5 K gauss. A stainless steel electrode had previously given an erratic, much lower average x-ray yield varying from 1.5 Kev at B = 3.15 K gauss up to 250 Kev at $B \simeq 5.3$ K gauss. The cause of the dependence of x-ray amplitude on the electrode surface is not known. There is some indication that the small neutron yield observed (for $B < 4$ K gauss) is higher for an Al surface than for brass. The x-ray lifetime and relative trapped x-ray signal (amplitude 100 μ sec after injection normalized by the initial signal amplitude) are found to vary slightly with changes in the gun supply bank. For input energies < 2.4 K joules at 4.3 K gauss the x-ray (e-folding) lifetime is ~225 μ sec, but for 3 K joules the lifetime drops to 171 μ sec indicating a degradation due to impurities or an increase in cold plasma density.

3-8.4.2 PLASMA STUDIES. Emphasis has been placed on the confined plasma. Utilizing the new energy source, the deuteron distribution has been measured at the ring cusps and found to duplicate earlier data. Measurements taken at the output cusp indicate several plasma reflections (2 or 3) occur prior to sudden decay cut-off at ~20 μ sec. It is hoped that an increase in the amount of plasma and confinement time can be achieved for deuteron energies in the range 1 to 10 Kev.

3-8.4.3 PLANS. The use of ions or electrons to measure the plasma potential (ϕ) is planned. A device with larger magnetic field and dimensions is being considered as a replacement for PICKET FENCE II B.

3-10 PLASMA GUN RESEARCH.

3-10.1 LARGE BORE HYDROMAGNETIC GUN. A large-bore hydromagnetic gun, Figure 4-S,

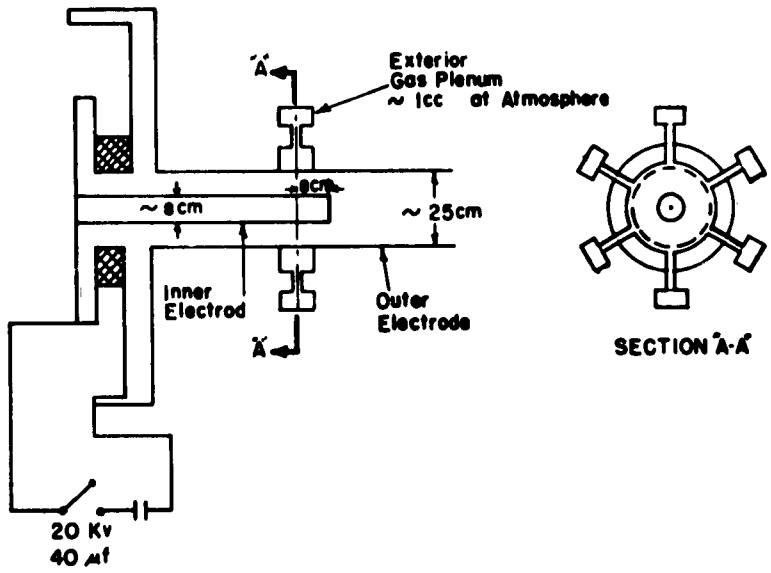

Figure 4-S. Large Bore Hydromagnetic Gun

has been set up and operated with the gas valve located on the outside electrode to facilitate geometrical changes in the inner electrode configuration. This gun has an insulator hidden from the radiation of the discharge that proved to be effective in discouraging breakdown at the breech. The gun was driven by eight 5μf, 25 Kv low-inductance capacitors each connected to the cable header with four low-inductance coaxial cables. The current rose in 1.5μsec when the header was shorted at the breech. Results with this gun indicate a reasonable neutron production. About 10^7 neutrons/pulse are produced in the vicinity of an end plate located 1.5 m downstream from the gun under typical operating conditions. The yield is not strongly dependent on electrode diameter, measurements indicating little variation (less than a factor of 2) as the diameter is changed from 2.5 cm to 10 cm. For best operation, the gas distribution should be a maximum about 3 cm behind the end of the central electrode, although this also does not have a strong effect on neutron yield. Measurements of the position of the current sheath vs time, and Kerr cell photographs indicate that the deuterons which produce neutrons are accelerated at the same time as a fast pinch occurs off the end of the central electrode.

3-10.1.1 PLANS. A faster bank will be used to get a cleaner plasma. Emphasis will be placed on photography as a diagnostic technique.

3-10.2 COAXIAL GUN INJECTION INTO A MAGNETIC FIELD. Experiments are conducted with a plasma gun system which gives volume neutrons when its ejected plasma stagnates against a magnetic mirror. Two modes of operation are significant. In the first mode, when there are small delays between gas admission and gun voltage application, there are large yields of gun neutrons, small diamagnetic signals, a sharp kink in the current signal corresponding to production of gun neutrons, and an x-ray signal. In the second mode, when the delay time is optimum for stagnation neutron production, there are no gun neutrons and no hard x-rays. The current rises for about 1 μsec and falls linearly to near zero in about 3 μsec. Large quantities of energetic plasma ($\sim$10 Kev) are produced.

3-10.2.1 RESULTS. Attempts to increase the time of the neutron signal by symmetrizing the stagnation field were not successful. Similar attempts to measure the slow, low-β plasma component, with a Faraday cup behind a pinhole also failed. A reasonably quantitative, simple method of measuring plasma energy has been tested; it consists of measuring the current pulse induced in a coil by the injected plasma. A Rogowsky loop is used in the current connections, where, if desired, it can be threaded in the reverse direction through the leads to a dummy coil of similar characteristics connected in parallel to the same pulse current source. In this way the deflection due to the pulsed field can be bucked out.

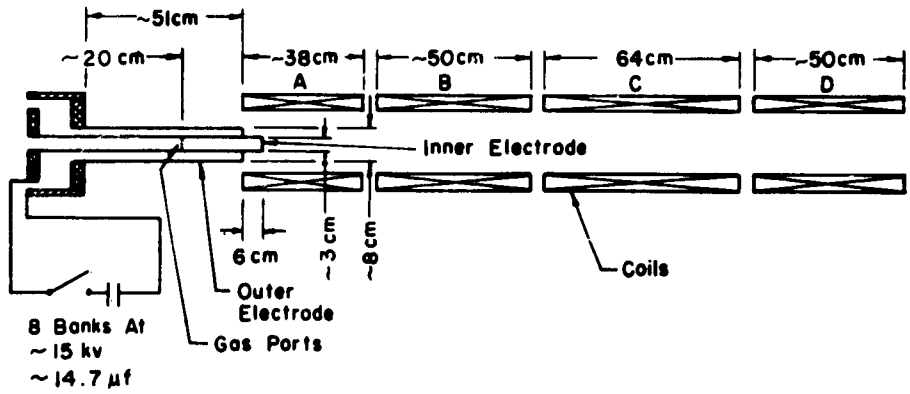

Figure 5-S. Coaxial Plasma Gun for Injection into a Mirror Field

SECTION IV

EXPERIMENTAL DEVICES AND RESEARCH AT THE LAWRENCE RADIATION LABORATORY

4-1. GENERAL. The most significant aspect of recent operation of the mirror machines at Livermore is the increasing experimental confirmation being obtained of the new "finite orbit" theory which explains stable and unstable modes of operation. If the theory is substantiated, it will permit designers to avoid known instabilities. TOY TOP III, for example, has been adjusted in length to take advantage of this theory and has apparently overcome the flute-type instabilities that were observed in previous models. TOY TOP 2X, now under construction, is designed to satisfy the stability criteria of this theory. ALICE, on the other hand, was constructed prior to the development of the theory and may have to be redesigned.

4-2. FAST NEUTRAL ATOM INJECTION EXPERIMENT: ALICE. Recent observations indicate that the fraction of the ionization that occurs due to Lorentz force is greater by a factor of five than it was previously thought to be. Tests have been made recently with the magnetic field at various values between 30 and the 50 Kgauss design level and with low density trapped plasmas, $1 - 2 \times 10^{8}$ ions cm^{-3}, in connection with the improving of diagnostic techniques and beam collimation. The device has a beam current of 60 milliamps, base pressure, 10^{-10} mm Hg, and operating pressure, 10^{-8} mm Hg.

4-2.5 PLANNED MODIFICATIONS. An axial ion gun is to be installed which will increase the beam intensity sixty percent and will allow the use of mixed deuterium and hydrogen in any desired proportions. The present offset ion source will be retained. The vacuum pumping capability will be improved to reduce the pressure toward the operating goal of 10^{-9} mm Hg.

4-3.5 TOY TOP III S. The pulsed-field coil system of the TOY TOP multiple-compression machine has been completely rebuilt. The new coil structure has a 9-inch instead of the 6-inch tube previously used, produces a smoother and more symmetrical field, and has a rise time of about 60 microseconds instead of 270 microseconds. The new arrangement is comparatively short and consists of only two stages. The symmetry of the magnetic field is such that the contour lines at the 9-inch diameter are circular within ± 0.13 inch. Deviations from symmetry of the magnetic surface which bounds the plasma are less. The III S system was operated and neutrons were observed. Attempts were made to increase the reaction rate so that it could be followed better as a function of time. The transport of plasma from the interior of the confining field across the magnetic field to the vacuum chamber walls was eliminated successfully. However, the rate of neutron production still decays with the apparently invariable 50 to 70 microsecond time constant. To date, it has not been possible to explain the decay as being due to hydrodynamic instabilities. The object of current research is the understanding of this decay and the increasing of the time constant.

4-3.6 TOY TOP 2X. Much of the construction has been completed and TOY TOP 2X will be operating for field symmetry adjustments early in fiscal year 1964. The dimensions of 2X are twice the linear dimensions of the earlier TOY TOP. Much more diagnostic equipment has been included. The plasma density and the magnetic field will be about the same but the volume of the contained plasma will be up to ten times as great as in the earlier TOY TOP.

4-4.3 TABLE TOP III RESULTS. A continuing effort has been made to reconcile both the observed stability and the observed unstable plasma behavior with theory. It has been confirmed that the same type of rotating flute seen with a "hot electron" plasma has been seen with a "hot ion" plasma, except that in the latter case the flute is observed to rotate in the opposite direction, that is, in the sense expected if the plasma potential is positive. It appears that the rotating instability occurs whenever an unstable condition is detected and when the rotating flute is not present no other instability is operative. High-mode-number flutes are not observed. Nonlinear effects are important; the growth rates of the instability, for example, do not seem to be as rapid as simple theory would indicate. Also, definite evidence is observed of instability "triggering thresholds" or of shock-like phenomena which sharpen the shape of the rotating flute. In many cases it has been observed that the instability, accompanied by rapid radial diffusion, may begin only to disappear before the plasma reaches the chamber wall. A recent study of the plasma shape and motion during an instability was made using eight scintillators located outside the mirror and intercepting the end scattered electron flux. An instability was triggered using a pulsed axial magnetic coil. The plasma left the axial position and spiraled outward. Scintillator signals indicated that the plasma had the shape of a column of roughly circular cross-section. The average column radius was about 2 cm, and the average radial velocity was about 5×10^5 cm sec^{-1}. A mechanical analog was constructed to aid in the interpretation of the electrical signals from electrostatic (capacity) probes placed near the rotating plasma. The mechanical model consisted of a charged disc (simulating a section of the column of plasma) rotated about an offset axis (simulating the rotation of an unstable plasma column about the central axis of the mirror machine) and an electrostatic probe. The charged rotating disc and the disc of the electrostatic probe form a variable capacitor. When the electrical time constants of the associated circuits were adjusted in proportion to the ratio between the observed period of plasma rotation and the period of the model, the waveforms of the electrical signals from the probe near the disc showed excellent agreement with those from the probe near the plasma. Information from the signals obtained showed the plasma potential to be negative in the case studied and that the plasma form could be a circular disc of radius ≤ 3.5 cm.

4-5 ASTRON. A self-consistent solution for the distribution of electrons in an infinitely thin E-layer has been derived analytically. This model of the E-layer does not exhibit the axial bunching instability or the B_θ instability during buildup. The ampere-turn distribution at the ends of the confinement region needed to produce the desired fields in the E-layer region has been derived from this model.

4-5.3 STATUS. The ASTRON reactor chamber is presently under vacuum; four of the six accelerator units have been installed, a fifth has been assembled and the sixth is being assembled. The control console is under construction. The requirement for a precise "flat top" pulse feed into the electron gun has received considerable attention. A test stand program to check out components is running concurrently with ASTRON fabrication. For the purpose of determining some of the natural resonant modes of electromagnetic energy propagation in the ASTRON tank and finding means to suppress or change the more dominant of the modes, a one quarter scale model of the tank is being constructed. The size and mechanical design of the model will allow frequent disassembly for experiments with internal structure and mode-suppressor design. Full operating condition of the ASTRON facility is anticipated in February 1964.

4-6. LIVERMORE PINCH EXPERIMENTS. An elementary theory of the finite-conductivity stability problem has been formulated. It predicts three basic types of resistive instabilities: A long wave tearing mode corresponding to the break-up of a current layer along current flow lines; a short wave rippling mode due to the flow of current across the resistivity gradients of the layer; and a low β, pressure driven interchange mode that grows in spite of finite magnetic shear. The predictions of the present theory appear to fit known experimental results. Using the finite-conductivity theory, efforts to correlate experimental and theoretical stability results are being accelerated. The specific experiments concerning resistive instability are:

a. A hard-core pinch experiment with an outer cusp field to study the importance of field curvature.

b. A TRIAX or resistive sheet pinch experiment to study the tearing instability.

c. A large, new, hard-core pinch experiment with special diagnostic equipment to study the rippling and tearing modes.

d. The LEVITRON experiment to study plasma containment under conditions satisfying the finite conductivity theory and thereby to provide information on the rippling mode and the pressure driven resistive mode.

4-6.5.1 12 INCH LEVITRON. A high powered LEVITRON of 12 inch bore designed for high purity plasma and high temperature operation was completed in April 1961. Failure of the vacuum system necessitated disassembly in August 1961. The difficulties have been overcome, and new vacuum pumps with 10 times the capacity of the present pumps will be installed. A hollow-cathode-discharge plasma source for the LEVITRON has been constructed. The source operates in a radial port and injects plasma onto flux surfaces as they are swept inward. A thermionic cathode is used. Pulsed D_2 is injected into the hollow tubular cathode region and a 50 to 100 ampere discharge is formed to a tubular anode. LEVITRON operates at an electron energy of 50 ev and a plasma density of 5×10^{13} ions cm^{-3}. New magnetic field probes will be added to determine the radial distribution of the B_θ and B_z fields. Planned work includes electron energy experiments, microwave experiments, and high energy plasma injection experiments.

4-7.6 ROTATING PLASMA RESEARCH: HOMOPOLAR V. This device was operational for the first time in January 1962, Figure 6-S. The main improvements over HOMOPOLAR IV are in the vacuum system, the magnetic field coils, the deuterium container, and a fast acting valve. The magnetic field coils are stronger, more flexible and allow operation at higher magnetic fields. The deuterium cavity is located in the center of the apparatus and is cylindrical. The gas release is radially symmetrical and it is believed that it is because of the change in shape and position of the cavity that nearly all of the tests now show a backvoltage whereas less than one-third showed a backvoltage in HOMOPOLAR IV. A new fast acting valve has proved more reliable than the one previously used. The electrode structure is identical to that of HOMOPOLAR IV. Typical operating characteristics are: volume of D_2 injected, 30 to 50 microliters; ion density, 10^{14} to 10^{15} ions cm^{-3}; total neutrons produced, about 10^5; randomized ion energy, 4 to 5 Kev, nearly all of which is in the ions. Most present experiments are for the purpose of improving diagnostics. Attempts to detect neutrons resulting from the D-D reaction have been unsuccessful in the past because of the γ-ray background produced by the device. Scope pictures of the scintillation detector output pulse shapes have been used successfully to

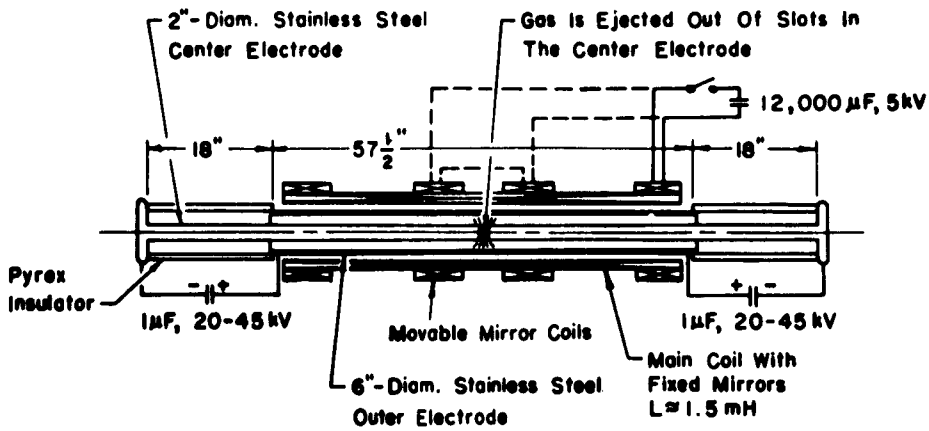

Figure 6-S. Schematic Diagram of HOMOPOLAR V Device

discriminate between the neutrons and the γ-rays. It is planned to use a pulse shape discriminator circuit in connection with a stilbene crystal and a photomultiplier for the purpose. Both the electrical and magnetic inputs will be increased. An electrolytic, 0.25 megajoule capacitor bank is now in use.

4-7.7 HOMOPOLAR VI is now on vacuum pumps; the pressure has been reduced to 10^{-8} mm Hg. The machine will be operated first as a single ended device starting probably in February 1963.

4-7.8 PLANS. It is planned to use the HOMOPOLAR principle in a plasma gun. A gun using this principle may be superior to the coaxial plasma gun.

4-7.9 HOTHOUSE III. This ion cyclotron resonance heating apparatus is in limited operation, Figure 7-S. A conducting screen was added at the end of the apparatus and perpendicular to the magnetic field in order to control turbulence. Further, the slow bank ionizing voltage was applied to the same electrode that supplied the wave-inducing rf field, thus freeing the opposite end of the apparatus to accept the conducting screen. Some wave-field measurements made earlier were repeated with the conducting screen in place. The screen substantially reduced the time dependence of the B_θ wave-field amplitude indicating that the turbulence associated with the wave-propagation was reduced. Application of a 9 Mc radial electric field to the coaxial electrodes produces a predominantly torsional hydromagnetic wave in which the azimuthal component, B_θ, is approximately proportional to $1/r$ at the electrodes. As the wave propagates down the tube, the total wave energy per unit length and hence the wave amplitude rises because of the spatially decreasing magnetic mirror field and the consequent drop in wave velocity. The energy per unit volume is only slightly decreased by the increasing area of the wave front. As the resonance region at the mirror center is approached, most of the energy of the wave is converted into thermal energy in the plasma. The efficiency of power transfer from the oscillator to hydromagnetic wave motion is approximately 50 percent. About 95 percent of the energy of the wave is transferred to the highly ionized plasma in the ion cyclotron resonance region at the mirror center. Normal operation is at 0.5 megawatt. The apparatus was shut down early in January 1963 for the addition of a stainless steel liner which will be run hot (at about 600°C) to reduce the losses due to contaminants entering the tube from the walls during operation.

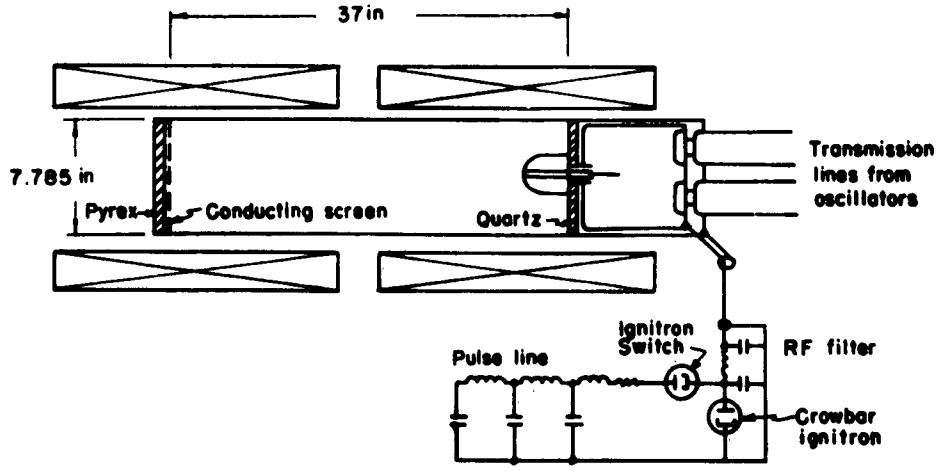

Figure 7-S. Schematic Diagram of Modified HOTHOUSE Apparatus

5-2.3 DCX-1 OPERATION WITH CARBON ARC. Instead of 2.7 Mw accepted by each coil on DCX-1, 3.5 Mw is the total power available in the four field coils. Instead of 25 micro-inch nickel foil, 10 micro-inch foil is now used on the neutral particle detector.

5-2.5 RESULTS. Recent experiments have been primarily studies of the characteristics of plasma established by low pressure gas dissociation of the incoming H_2^+ beam. Measurements of slow plasma currents drifting to insulated end walls positioned outside the throats of the mirror coils indicate that the primary source term is ionization of the background gas by trapped protons, Figure 8-S. Simultaneous measurements have been made of these currents, the intensity of rf activity, the plasma potential (by the lithium beam technique), and signals to neutral particle detectors (NPD). Coincident with the bursts of rf activity there are fluctuations in the electron current out of the mirrors, increases in plasma potential by as much as several hundred volts, and sharp increases in signals to the NPD. At the cessation of rf the current fluctuations cease, the plasma potential drops, and the NPD signals gradually recover to steady-state values. An explanation is that the heating rate for electrons in the plasma increases with rf activity, the plasma potential then increases in order to balance the loss rates of slow ions and electrons, the energy loss rate of the fast circulating protons increases, and these additional losses are reflected in a higher charge exchange loss rate. Studies of the various field components of the rf signals confirm the existence of charge "clumps" rotating with the trapped protons. Studies at low pressures have also shown the existence of a repetitive short burst activity involving purely longitudinal currents or electric fields. Injecting an electron beam into the plasma along field lines causes marked changes in the rf signals and in the energy distributions of the charge exchange neutrals. The injection of 400 Kev H_2^+ has been coupled with electron cyclotron heating in the plasma region. Although there is evidence for electron heating, the dissociation of the molecular ion beam was not enhanced by the modest power levels employed (about 5 watts).

5-2.5.1 PLANS. The on-off repetitive action of DCX-1 which has the effect of quenching fast proton instability, suggests deliberate disorder injection of the H_2^+ beam would produce a stabilizing effect upon the plasma ring (3.25 inch radius). As a result, experiments were set up to (a) inject the H_2^+ beam slightly out of the median plane and (b) inject the beam in the median plane but allow it to swing inside or outside the 3.25 inch H^+ stable orbit (plasma ring) so as to deliberately introduce more precession into proton orbits. It was found that this technique does tend to stabilize the system and will be investigated in detail.

5-2.6 WALL EFFECTS. The wider vacuum liner modification in DCX-1 has been completed.

5-3.7 STATUS OF DCX-2. All the principal components (the accelerator and injection system, including the shielded injection channel or "snout", the coils producing the tailored magnetic field, and the vacuum system) are in operation.

5-3.8 RESULTS. The DCX-2 apparatus is designed to produce an energetic proton plasma in a mirror magnetic field by dissociation of energetic H_2^+ ions over a long path in the magnetic field. DCX-2 has been operated with injection currents up to 40 milliamperes, H_2^+ current,

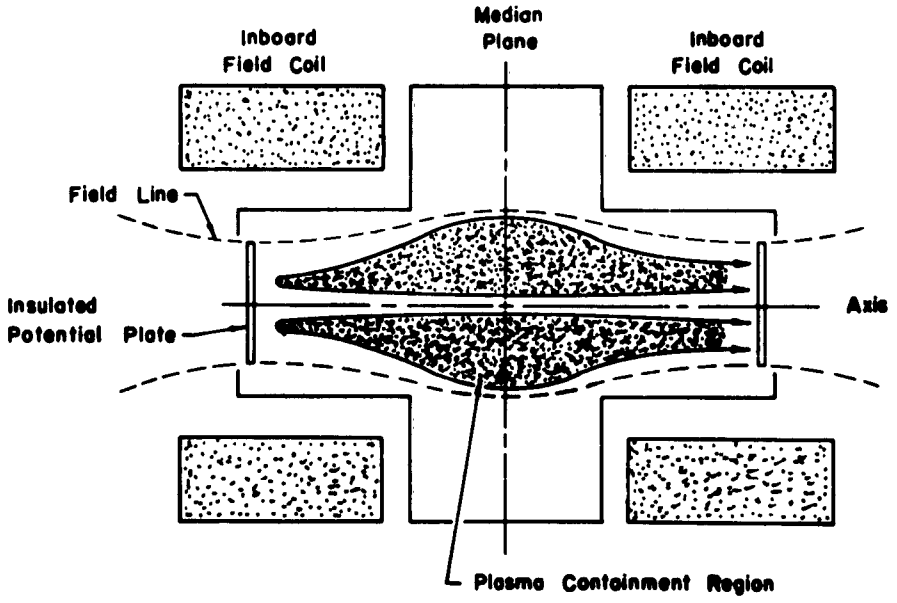

Figure 8-S. Slow Ion Plasma Drift in DCX-1

at 600 Kev. Complex plasma behavior was observed which limits the density of the energetic plasma. At turn-off, beam currents of neutral particles are observed emanating from the end regions of the machine which reflect a trapped ion density $\sim 10^7$ to $18^8/cm^3$ with a decay mean life of ~8 milliseconds. However, hot-ion densities of only $2 \times 10^6/cm^3$ are seen in the flat central region of the magnetic field. These plasmas decay following beam turn off with mean times not inconsistent with charge-exchange losses; however, with the beam on, the losses increase by a factor of at least 50 to produce the observed results.

5-4.2 RESULTS OF ELECTRON CYCLOTRON HEATING EXPERIMENT. Experimentation was performed using a continuous wave power source capable of applying up to five kilowatts of 10.8 gigacycle microwave power to the plasma. Figure 9-S shows the experimental arrangement. With the application of two kilowatts of power and using a deuterium gas feed neutron emission from the plasma was observed by a U-235 fission counter and validated by foil activation measurements. With the plasma adjusted for quiescent steady state operation, the neutron production rate is optimum. With the plasma adjusted for noisy unstable operation, the neutron production rate is sharply decreased. The U-235 detector indicated a source strength of $\sim 10^5$ n/sec at 2 Kw of microwave power when calibrated against a known Am-α-B neutron source. Further checks with a He^3 proportional counter showed that the neutron source strength increased roughly as the square of the applied microwave power. The He^3 counter detects neutrons through the reaction He^3 (n, p) T with a Q of approximately +770 Kev. Measurements of 8mm microwave noise amplitude and diamagnetic signal from an axial probe showed a similar dependence on microwave power. The neutron production took place only in a fairly narrow range of magnet current variation. The region of enhanced neutron emission and maximum noise amplitude was correlated with the microwave resonant heating zone positions near the mirror throats.

5-4.2.1 EXPLANATION OF RESULTS. The most reasonable explanation of the large flux of kilovolt neutrons from the electron cyclotron plasma (ECP) appears to be coulomb-or electro-dissociation of deuterium by high energy electrons (i.e., $e+D \rightarrow e + n + p$). Electrons with energies greater than the binding energy of deuterium are believed to be present in the ECP since x-rays with several Mev of energy have been observed. There is an insufficient amount of D_2 or Be in or near the device to produce the neutrons by (γ, n) processes and all other materials have too high a (γ, n) threshold to produce the observed neutron flux. Calculations show that the cross section for electro-dissociation at 3 Mev is $\sim 10^{-30}$ cm^2. Measurement at an electron energy of 3.8 Mev estimates the cross section to be in the range 10^{-31} to 10^{-30} cm^2, which is in substantial agreement with the above calculation. Using this cross section and a plasma volume of 10^4 cm^3, it is estimated that a high energy ($\gtrsim$ 3 Mev) electron population of $\sim 10^9/cm^3$ is required for the observed neutron emission rate. As the plasma density is $\sim 10^{12}$ $/cm^3$, this requires only a small fraction of the electrons to be in the energy group which produces the neutrons and is in substantial agreement with the observed x-ray flux measurements.

5-4.3 PLANS. A new larger device for plasma heating at the electron cyclotron frequency is expected to be in operation by April 1963. Lead shielding will be provided for protection against x-rays. The purpose of this device is to study the effect of using a larger confinement volume. It is planned to inject a 20 Kv, ~50 milliampere deuteron beam into the cavity. It is hoped that a hot electron "blanket" of sufficient size to insure neutral gas burnout will be produced. By the end of summer 1963 a 13 Kw continuous wave power source is expected to be available.

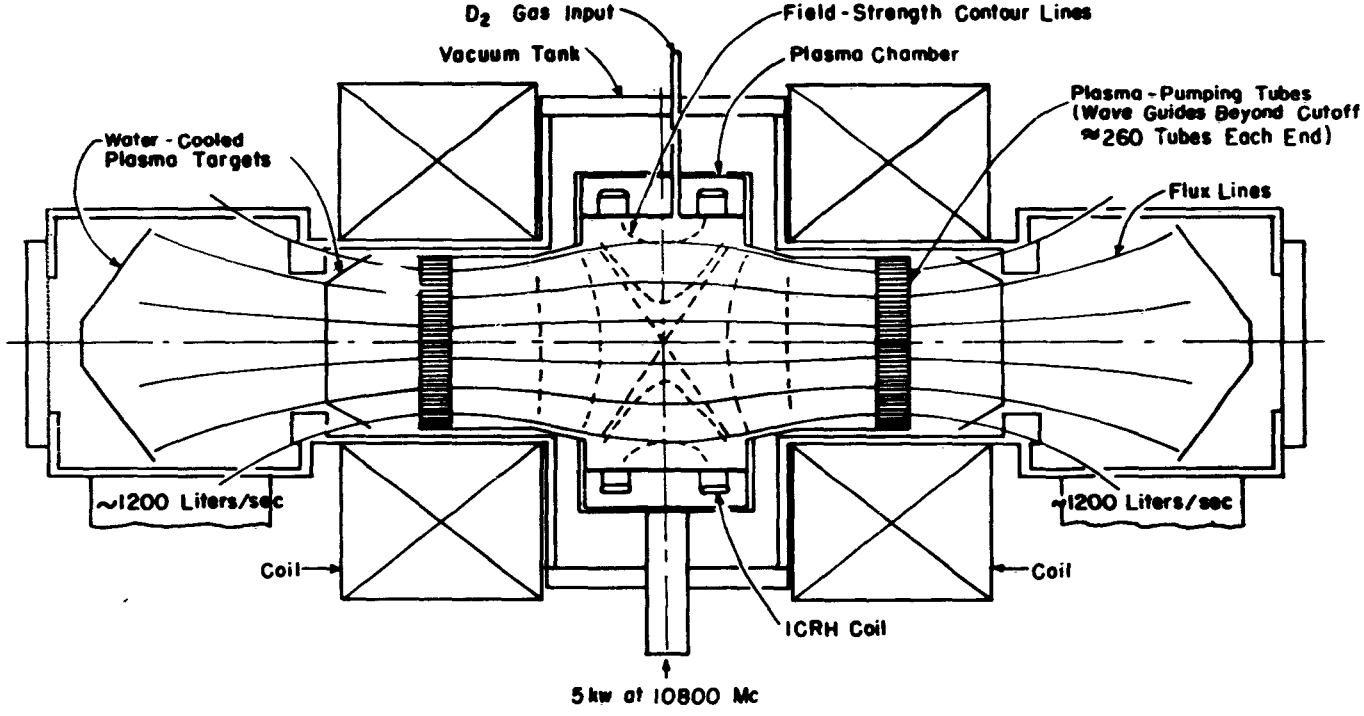

Figure 9-S. A Schematic Drawing of the Electron Cyclotron Heating Experiments

5-9. STUDY OF TRITIUM BLANKET REQUIREMENTS FOR A(D, T)REACTOR. Since the design details of a successful thermonuclear power device are not known, only the two principle functions of the blanket were considered; namely, (1) moderation and multiplication of the 14.1 Mev neutrons from a (D, T) plasma and (b) the breeding of tritium, Figure 10-S. The function can probably be most readily performed by fluid blanket components which will permit heat extraction at reasonably high temperatures. Factors considered were:

a. Provision for neutron multiplication.

b. Moderation of neutrons to low energy and their reaction with lithium-6.

c. Small parasitic neutron capture.

d. Absorption of secondary gamma rays.

e. Extraction of heat at useful temperatures.

f. Recovery of tritium.

g. Stability and chemical compatibility.

h. Compatibility of the blanket with magnetic requirements, small electrical losses.

i. The pressure of the system should be low at operating temperature.

j. Minimum induced radioactivity.

k. Minimum thickness.

5-9.1 CONCLUSIONS. Molten $LiF\text{-}BeF_2$ is a promising blanket material for removing energy from a thermonuclear reactor in the form of useful heat and for breeding tritium. In the interest of minimizing blanket thickness and of maximizing neutron multiplication, the possibility of including heavier elements such as lead, tin, barium, and zirconium in a fluoride salt mixture to be placed in one region of a blanket assembly should be considered. It is probably not too early to start to obtain information needed to determine the feasibility of employing molten fluorides in a thermonuclear reactor blanket. Some of the problems that need to be examined are: compatibility of molten fluorides with container and neutron multiplying materials and means of dealing with the corrosion problem resulting from charge imbalance accompanying tritium production, and solubility of tritium and tritium fluoride in molten $LiF\text{-}BeF_2$. Due to lack of information on the configuration of a successful thermonuclear reactor, it does not appear profitable to attempt blanket design studies at this time.

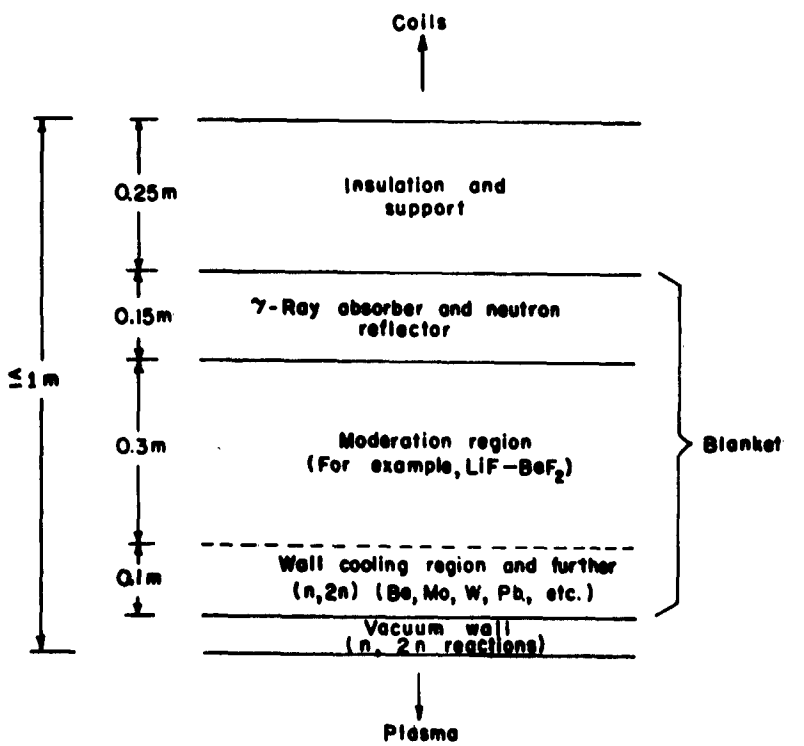

Figure 10-S. Schematic Blanket Design for a Thermonuclear Reactor

5-10. ELECTRON BEAM-PLASMA INJECTION EXPERIMENT. See Figure 11-S. Both the plasma and the electron stream were formed by a pressure gradient arc. The arc is produced by feeding gas into the aperature in the anode which defines the electron stream, producing a local region of higher gas pressure. When a stream of electrons passes through this higher pressure region, a dense volume of plasma forms inside the anode. In this experiment the cathode heating current is removed once the plasma is formed. Therefore higher negative bias may be applied since only the region of the cathode bombarded by ions is heated to emission. This plasma region extends into the space between the mirrors and emits energetic ions in random directions. An electrically floating anticathode electrode reflects the electron stream and produces a reflex discharge. X-rays were produced; however, the addition of a copper enclosure around the plasma region increased the x-ray photon yield by about a factor of 100.

5-10.1 RESULTS. Interaction between the electron stream and plasma of deuterium or helium resulted in heating of the plasma electrons. The resulting steady state plasma emitted x-ray photons with energies up to 250 Kev. From the photon energy distribution and total flux, an electron temperature of 32 Kev and density of about 4×10^{11} electrons cm^{-3} was indicated.

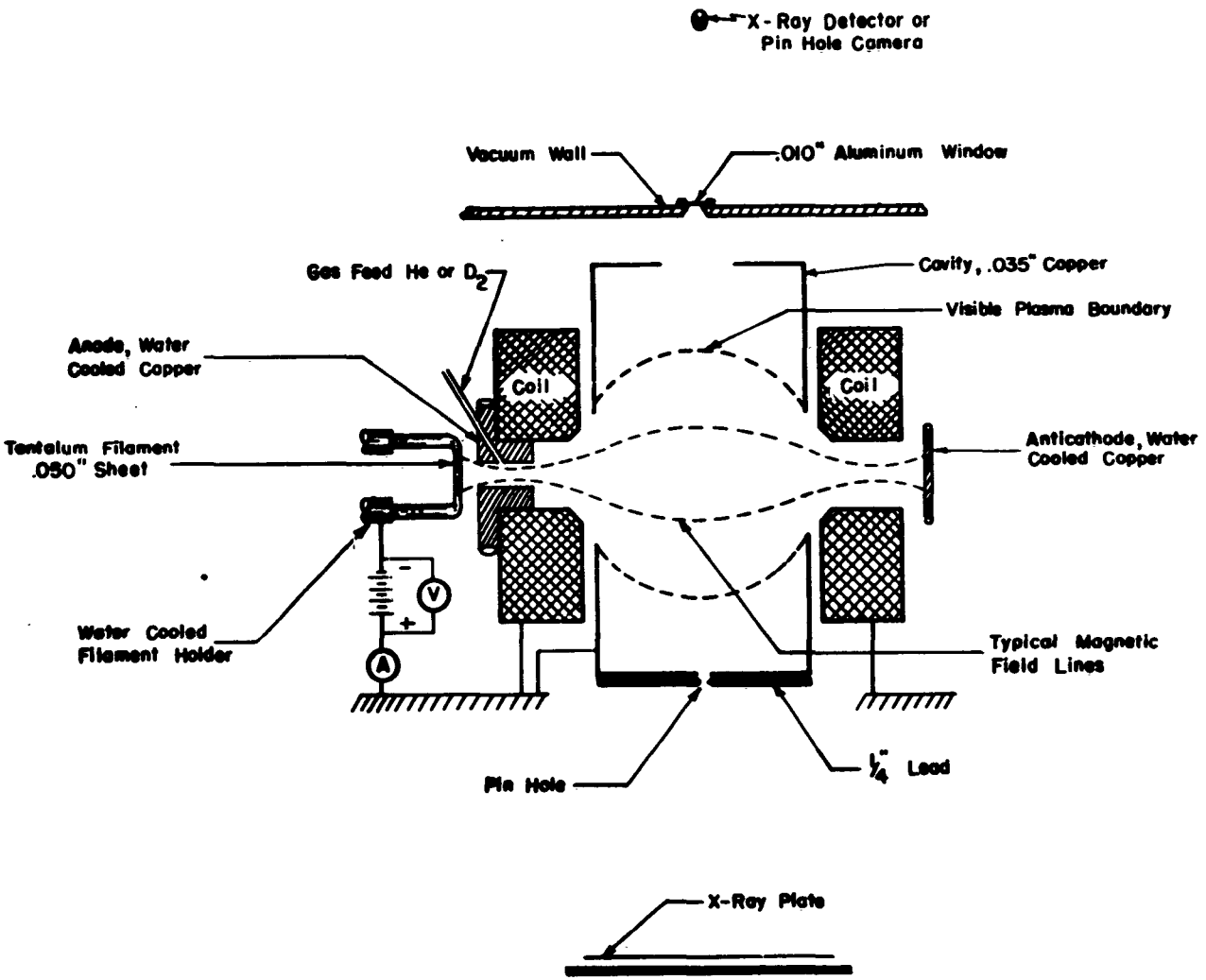

Figure 11-S. Sketch of Electron-Beam Plasma Injection Apparatus

SECTION VI

EXPERIMENTAL DEVICES AND RESEARCH AT PRINCETON UNIVERSITY

6-2. C STELLARATOR. After about one year of operation the C stellarator has begun full operation using shaped pulses for ohmic heating. Ion cyclotron heating will be introduced later in 1963 instead of the previously planned magnetic pumping which is now scheduled for 1964.

6-2.1 STATUS. The installation of field stabilizing windings, the divertor and ion-cyclotron heating equipment has been completed and is in operation.

6-2.3 MAGNETIC PUMP. Calculations predict that the low-Q capacitors to be utilized for magnetic pumping will provide insufficient energy for plasma heating. Because of the high-Q capacitors intended as replacements are still in the development stage, it was decided to install ion-cyclotron resonance heating of frequency range 7 Mc and 15 to 40 Mc; eventually to be improved upon with the use of Hard Tube Modulator for Audio-Frequency (HTAF) in the frequency range 40 to 200 Mc. The high-Q equipment is scheduled for 1964 installation.

6-2.5 DIAGNOSTICS. Of the two diagnostic instruments intended for ultraviolet spectroscopy work on C stellerator, the grazing incidence single-channel vacuum spectrograph has been emphasized because of the good data obtained. The six-channel, one-meter focal length spectrograph is still in preparation.

6-2.6 RESULTS. Experimental work on the machine was divided into three main categories as described below.

6-2.6.1 IMPURITIES AND OPTICAL RADIATION. The grazing incidence vacuum monochromator was calibrated and used to study time behavior and absolute intensities of lines of the stellarator working gas, (e.g., H, He) and of impurities in the spectral range of their strongest lines. The observed rates of ionization of the oxygen impurity from one state to the next, in conjunction with electron density measurements by microwave phaseshift, were used to obtain electron temperatures at various times in the discharge. Measurements of the relative line intensities of two or more transitions were used to calculate the electron temperatures. Such "excitation temperatures" were computed from measured intensities of several resonance multiplets of doubly and triply ionized oxygen using excitation cross sections. Temperatures obtained were in reasonable agreement both with the conductivity temperatures, and with the ion temperatures as measured from Doppler widths of the lines, although moderate discrepancies exist in the time behavior of the various temperatures. The temperatures were used in conjunction with the absolute line intensities to calculate the absolute concentration of the oxygen ions in the plasma as a function of time. The results indicate a rapid oxygen influx early in the heating current pulse followed by a net efflux with typical particle confinement times of the order of a few milliseconds.

6-2.6.1.1 RADIATION LOSS AND POWER BALANCE. An attempt was made to determine the power balance in the C stellarator by using the vacuum monochromator to measure the absolute power radiated from the plasma and comparing it with power input during the discharge pulse. Determinations were made using the normal operating gas (H) and helium impregnated gas.

Results indicate that for normal gas discharges the plasma is about 50 percent radiation-limited for low plasma currents of ~2 Kamp, but that the fraction of power going into radiation drops off as the current is increased and suggests an enhanced particle loss. In discharges containing helium as an added impurity the plasma is essentially completely radiation limited over wide ranges of plasma currents and magnetic confining field strengths.

6-2.6.2. STUDY OF PHENOMENA DURING OHMIC HEATING. Three experiments were conducted to determine (a) the effect of helical windings, (b) U-bend drifts, and (c) the effect of a transverse magnetic field applied over the entire C stellarator.

6-2.6.2.1 THE EFFECT OF HELICAL WINDINGS ON PLASMA BEHAVIOR. It was found that:

a. The helical windings introduce a rotational transform up to 58° at a radius of 5 cm.

b. The potential difference due to charge separation caused by U-bend drift is reduced.

c. When the ohmic heating (OH) current (J) unwinds the introduced rotational transform at the plasma boundary, the discharge becomes unstable.

d. If the lack of closure of the vacuum magnetic field (B_o)is removed and the stellarator is made symmetric,(paragraph 6-2.6.2.3) the helical winding reduces by a factor of 2 the applied voltage required to maintain a given plasma current indicating a higher temperature.

e. The "runaway" effect of a deliberately introduced lack of B_o field closure is minimized by the helical windings.

6-2.6.2.2 PLASMA DRIFT AT THE U-BENDS IN C STELLARATOR. With no helical transform, potential differences of several tens of volts between the top and bottom of the plasma at the U-bend indicates that charge separation takes place. This difference changes sign if the direction of the magnetic field is reversed while the other variables are kept constant. Density profiles show that the plasma does not touch the tube wall for high confining fields if an aperture limiter (short-circuiter used to decrease the perpendicular electric fields in the plasma torus) is inserted. With the helical transform, plasma is nearly centered in the aperture limiter.

6-2.6.2.3 THE EFFECT OF A TRANSVERSE MAGNETIC FIELD. It was discovered that the confining field, B_o, failed to close by 0.26 cm. This asymmetry was corrected by imposing a transverse magnetic, B_t, over the entire stellarator and resulted in significant improvement of the energy replacement time, τ_E, and particle confinement time, τ_p, . Further, improvement of τ_E and τ_p, as well as a reduction in the plasma diameter and better centering of the plasma in the aperture limiter, is obtained by adding an extra component of vertical transverse field (~10 gauss) in addition to that required for symmetry. This extra field depends upon the plasma current and is required to (a) balance the magnetic confining field drift in the U-bends with a $J \times B_t$ force and (b) balance the hoop force (force created by the OH current flowing toroidally in the plasma).

6-2.6.3.1 NEUTRAL DENSITY VARIATION. In the ionization phase of stellarator discharge the density of neutral hydrogen molecules is reduced by dissociation and ionization. By programmed OH pulses, the ionization is completed in a few microseconds and the plasma is then

held at ~ 1 ev for ~20 msec during which time the electron density decreases (afterglow). At this low temperature it is not expected that recombination would occur in the plasma nor that molecular hydrogen returned to the volume from the walls would be ionized. The OH pulse ionizes the neutral gas and the resulting plasma increase is taken as a measure of neutral density. Fast ion gauges to measure directly the neutral pressures have also been used. Results indicate that neutral atoms produced during the initial dissociation remain for 5 to 8 msec. Charged particles recombine at the stellarator walls and the rate of return may be slower or faster than the rate of neutral return, depending upon discharge conditions.

6-5.1 STATE OF B-1 STELLARATOR. Conversion of this device for use in a new set of experiments is complete and it has been used to study wall effects and plasma impurities.

6-5.2 RESULTS. Aperture limiters were used across the beam to study impurity effects. By inserting a limiter it was shown that wall impurities decreased; however, a large contribution from the limiter itself was detected. This observation was made from the output signal of a monochromator under fixed conditions.

6-5.3 PLANS. More significant data in terms of ratios of impurity signals to He-II signals will be taken as soon as improvements of the optical system are completed. A study of the impurity release from different surfaces by varying the limiter material and treatment is planned.

6-6. B-3 STELLARATOR. In addition to the conventional and HTAF ohmic heating available a new 25 Kw magnetic pump in the ion-electron hybrid frequency (500-600 Mc) range has been added.

6-6.1 INDUCED ELECTRIC FIELD. Current-voltage characteristics of simple, wire-type Langmuir probes have been obtained as a function of position and time in nearly fully ionized hydrogen plasma. The confining field was up to 38 K gauss; n was 5×10^{13} cm^{-3} and conductivity temperature was 15 ev. Well-defined saturation current densities for both ions and electrons in the ratio of 1 to 30 were discovered. If too large an electron current is collected on the probe a radial electric field as high as 300 v/cm can be induced in the plasma indicating that a plasma capacitor is established having a magnetic surface as the inner plate, the discharge tube as the outer plate and the plasma as the dielectric.

6-6.2 PLASMA LOSSES. Profiles taken under three different conditions indicate nearly cylindrical conditions exist for the space potential and ion density. For these cases, a diffusion coefficient of $10^3 cm^2/sec$ was observed for the outer region for a 4 ev plasma in the 38 K gauss field. If the loss in the inner region, where no radial electric field exists is described by diffusion, the coefficient would be at least five times greater. More likely a drift causes the high loss in the inner region of this low temperature plasma. Computations show that an increase of a factor of 2 in the confinement time can be obtained by increasing the outer region in which the radial electric field is established.

6-8.1.1 ION ENERGY DISTRIBUTION IN B-66. The voltage induced in a loop by the diamagnetic field is proportional to the rate of change of perpendicular plasma pressure. Plasma temperatures obtained from this measurement and averaged over ~25 cm of the axis ranged between 100 and 180 ev for electron densities of $\sim 3 \times 10^{13}$ cm^{-3}. Temperature measurements made with a mass spectrometer employed to analyze the energy of ions escaping through a mirror in a magnetic beach were in general agreement with energy ranges from 20 to 150 ev. The low temperature of 20 ev indicates that most of the plasma pressure is due to ions. Measured decay times range from 10 to 80 microseconds.

6-8.2 NEW EXPERIMENTAL ARRANGEMENT. A new experiment is being prepared to determine if ion cyclotron waves can be propagated around U-bends. If successful, this will mean that it will not be necessary to incorporate a magnetic beach near the plasma source on C stellarator, but instead that it can be used in the divertor.

6-10. THE L-2 EXPERIMENT. The L-2 device is temporarily inactive.

6-11. THE Q-1 PROGRAM. Formerly called the Q Device, Program A, the device has undergone extensive modifications and is now in operation. No results are available.

6-12. THE Q-3 PROGRAM. This experiment was formerly called the Q Device, Program B.

6-12.1 RESULTS. Ion acoustic waves were excited in highly ionized cesium and potassium plasmas (5×10^{10} cm^{-3} < n < 5×10^{11} cm^{-3}) by modulating the potential of a tungsten grid immersed in the plasma. The waves are detected by a similar grid, which can be moved along the plasma column. Phase velocities are 1.3×10^5 cm/sec for cesium and 2.5×10^5 cm/sec for potassium with no measurable dispersion and are 70 percent in excess of those predicted for a collisionless plasma with equal ion and electron temperatures; $V_{ph} = \sqrt{4kT/M_i}$, T = 2300° K. The wave damping distances were observed to be independent of density and are a constant fraction of a wave length. The measured damping distances (~0.6 wave length) are ~50 percent greater than predicted.

6-13. PLASMA INJECTION EXPERIMENT. A device, Figure 12-S, has been fabricated to study the transverse injection of plasma by coaxial gun (similar to the PICKET FENCE, MARK II B Gun) into a bottle with fields up to ~ 18 K gauss. The purpose of the experiment is to determine (a) how much plasma is trapped, (b) at what energy and (c) in what proportion. Since gun output is known in detail, it will be possible, using the energy analyzer, to compare the amount of trapped plasma with output. Other diagnostic techniques include probes and microwave and frequency measurements.

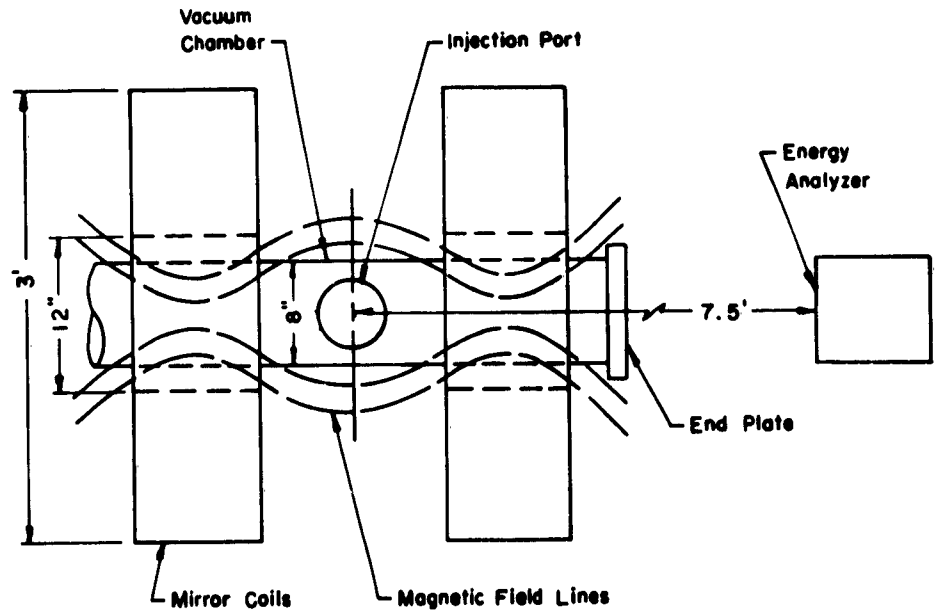

Figure 12-S. Plasma Injection Experiment

SECTION VII

OTHER EXPERIMENTAL DEVICES AND RESEARCH IN THE UNITED STATES

7-6. EXPERIMENTAL DEVICES AND RESEARCH AT THE MASSACHUSETTS INSTITUTE OF TECHNOLOGY.

7-6.3 ELECTRON BEAM-PLASMA INTER-ACTION EXPERIMENTS. An electron beam-plasma interaction experiment, Figure 13-S, studies electron beam discharges in helium and was concerned with (a) large-amplitude current oscillations of a few tens of megacycles (regime 1) and (b) emissions characterized by light, x-rays, kilomegacycle rf radiation, and the flow of ion currents to the wall (regime 2). At low pressures, the large-amplitude current oscillation extends throughout the pulse; as pressure is increased, the oscillation stops and emission begins

7-6.3.1 RESULTS. In regime 1, the power delivered to the beam was 11 percent less than the power delivered under high vacuum conditions. In regime 2, the power was 30 percent less than under high vacuum conditions. Results are summarized below.

REGIME	PRESSURE (mm Hg)	BEAM Voltage (Kv)	INDUCTION (Gauss)	I COLL (amp)	POWER (Arbitrary Units)
High vacuum	5×10^{-7}	10	324	0.55	10.0
1	8×10^{-5}	10	324	large oscillation	8.9
2	2×10^{-4}	10	324	0.65	7.0

7-6.4 FUSION REACTOR BLANKET. Final results of the fused lithium and beryllium flouride blanket mock-up to determine if tritium can be produced at a fusion reactor site indicate that a net production is possible. A tritium regeneration of ~1.2 was observed from the following reactions:

$$Li^6 + n \text{ (slow)} \rightarrow T + He^4$$

$$Li^7 + n \text{ (fast)} \rightarrow T + n + He^4$$

Calculations indicate that blanket thickness cannot be appreciably reduced below 1 meter and that it will probably have to be a rather long device in order to cut out end losses. The salt, $Li_2(Be\ F_4)$, appears to look best for use in a fusion blanket.

7-6.4.1 REACTOR BLANKET WITH FISSILE NUCLIDES. A study was initiated to explore the feasibility and merits of including fissile nuclides in a fusion blanket. The nuclides of primary interest are Th-232 and U-238. The advantages of using fissile nuclides in a blanket are (a) an increase in the power output of the system by virtue of the high energy fissions induced; (b) breeding of fissionable nuclides by neutron capture in either thorium or uranium; and (c) improvement of neutron economy of the system because of high neutron yield of high energy fissions. Disadvantages anticipated are (a) possible increase in the severity of salt corrosion;

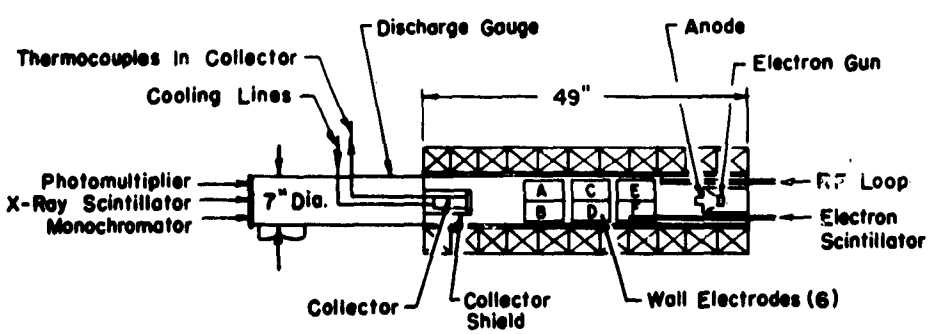

Figure 13-S. Electron Beam-Plasma Interaction Experiment

(b) severe radiation damage if the fissile nuclides are in solid form; and (c) increased radioactivity resulting from fission products. A 14 Mev Van de Graaf accelerator was used to irradiate 18-inch stacked discs (simulated walls) of varying thickness. The various discs were analyzed chemically. Results are tabulated below.

FIRST WALL				
Composition	Mo	Mo	Mo	Mo
Thickness (cm)	2.50	1.00	2.50	1.00
COOLANT				
Composition (Mole %) (LiF-BeF_4-UF_4)	73-00-27	73-00-27	60-30-10	60-30-10
Thickness (cm)	6.68	6.68	6.25	6.25
RESULTS				
Fission Rate	0.051	0.066	0.021	0.027
U-238 Multiplication	0.222	0.291	0.092	0.120
U-238 Absorption	0.246	0.231	0.111	0.101
Total Neutron Leakage	0.076	0.088	0.079	0.093
T Regeneration Ratio	1.050	1.070	1.080	1.070

The attenuator wall was 49 cm thick and contained 79% (66 LiF-34 Be F_2) and 21% graphite.

7-6-15 LASER-ELECTRON SCATTERING EXPERIMENT. In order to establish the feasibility of using a laser beam as a diagnostic tool for plasmas, preliminary experiments to observe Thomson scattering from an electron beam were prepared. By observing the scattered radiation at a suitable angle with respect to the electron beam, signals were obtained that are characterized by large Doppler shifts. These are easier to detect against the low background illumination than is a distribution that is spread out and centered about the transmitted frequency, as would be the case for a stationary and luminous plasma. The apparatus consists of a vacuum chamber in which a ruby laser beam intersects an electron beam at normal incidence. The region of intersection is observed through an optical system, which includes a photodetector, whose optical axis makes a fixed angle with the axis normal to the plane containing the beams. The observing system, however, can be rotated around that normal axis to allow observation at a variety of angles; therefore, different values for the Doppler shift can be obtained. At present, an

interference filter to obtain the spectral resolution is used and it is planned to use a grating monochromator. A 50-joule laser beam, at $\lambda \approx 6934$ Å, and an electron beam of 100 ma at 2 kv are being used.

7-7. EXPERIMENTAL DEVICES AND RESEARCH AT THE NAVAL RESEARCH LABORATORY.

7-7.5 ASYMMETRICAL DRIFT IN THE PHAROS COIL. In an effort to alleviate the anomolous plasma drift observed in PHAROS several pieces of shaped metal were placed between the plasma cavity and the lead header plates in an effort to achieve stability. Cylindrical end pieces were also used. All efforts failed. The plan to incorporate SCYLLA III-like multipoles to prevent plasma losses to the wall failed because the large magnetic forces generated caused the multipole wires to smash the vacuum tube. Efforts to use slots were, accordingly, terminated with the emplacement of the multipole wires in a plastic and fiber glass sheath to protect the vacuum tube.

7-7.6 RESULTS. Effort is continuing with x-ray diagnostics in order to calibrate measurements by passing the x-rays through several absorber foils to a scintillator coil. The purpose of this effort is to reduce the uncertainty of the reported electron temperature (350 ± 50 ev) in PHAROS.

7-7.8 PORTABLE POWER SOURCE EXPERIMENT. A new low inductance (50 nanohenry), 50 Kjoule (20 Kv, 250 μf) portable capacitor bank has been fabricated and will be used to produce x-rays in a theta pinch coil. Each of the 30 capacitors has a low inductance cable and switch (compared to one switch per each 3 capacitors on PHAROS); the bank is capable of producing currents up to 2 megamperes in the coil. Operating pressure is $\sim 10^{-7}$ mm Hg. The purpose of the experiment is to measure x-rays spectroscopically over a wide range with a variety of crystals. The vacuum system is operating now. The spectroscope will be assembled by Spring 1963.

7-8. EXPERIMENTAL DEVICES AND RESEARCH AT STEVENS INSTITUTE OF TECHNOLOGY.

7-8.2 CHALICE. The device is being dismantled and reassembled in a new location so as to provide a new low inductance (~1 to 1.5 nanohenries) capacitor bank of 80 to 100 Kjoules. Each of the two banks are designed to provide 50 Kv at 32 μf. Low inductance lines and switches are being fabricated for installation.

7-8.2.1 RESULTS. Experiments conducted at 30 Kv and 60 to 800 microns of Hg with a hydrogen plasma indicate the "plasma bounce" does not exist in high magnetic cusp fields (~25 Kgauss). Mixing in the cusp region is thorough and appears to be squeezed into a "pancake" which leaks out of the confinement region along field lines in the vertical median plane.

7-8.5 ELECTRON BEAM EXPERIMENTS: MEGATRON. A new 20 Kv capacitor bank is being assembled for use with the device. A small pilot model is in operation at the present time.

7-8.6 CESIUM PLASMA EXPERIMENT. The cesium plasma device operates at $\sim 3 \times 10^{-6}$ mm Hg and produces a plasma of better than 50 percent ionization with a density of 10^{11} particles per cm^3 in an 8 K gauss field. The magnetic field varies about 4 percent from uniformity with 5 coils and ~2 percent with 6 coils in operation (total length 16 inches).

7-8.6.1 RESULTS. Working at 5 K gauss and ~600 amps, x-rays were detected from a target deliberately introduced into the plasma. An interaction experiment to detect and observe Alfven waves is planned.

7-9. MAGNET DIPOLE EXPERIMENT. A device has been fabricated to simulate the magnetic field of the earth. Plasma flows around the dipole and is trapped in the magnetic vortices, i.e., ion density shows up as "islands" in the cusped field. It is planned to go to a quadrapole configuration.

SECTION VIII

EXPERIMENTAL DEVICES AND RESEARCH IN FOREIGN NATIONS

8.3 EXPERIMENTAL DEVICES AND RESEARCH IN THE FEDERAL REPUBLIC OF GERMANY.

8.3.3.3.1 THETA PINCH IN A FIGURE 8 STELLARATOR. The results of investigations of a theta pinch in a Figure 8 stellarator geometry revealed that plasma equilibrium behavior does not differ from that of a toroidal geometry stellarator.

8.3.4.1 ELECTRODELESS ACCELERATION OF A PLASMA. Hydrogen plasma injected by an electrodeless conical plasma gun into a 2 meter long vacuum tube was analyzed with magnetic probes and loops and with a retarding field spectrometer. At low gas pressure and magnetic field inside the conical coil, plasma was emitted at the start of the first half-cycle with an axial ion energy of 0.3 to 2 Kev. At higher pressures emission occurred in the second half-cycle with ion energy of 200 to 400 ev. Trapped magnetic fields occur during the first half-cycle and are believed to be the cause of delay of emission until the second half-cycle at high pressures.

8-4. EXPERIMENTAL DEVICES AND RESEARCH IN THE UNITED KINGDOM.

8.4.2.1.2 RESULTS. A new method for estimating electron temperature of hydrogen plasma in the ZETA and CUSPED COMPRESSION devices depends on the temperature variation of the intensity ratio of the continuum radiation on both sides of the Balmer (ZETA) and Lyman (CUSP) series. Difficulty encountered in the method was caused by impurity spectural lines, hence the accuracy of ZETA measurements was only a few percent for temperatures less than 10^{5}° K. Reasonably consistent results have been obtained for the Lyman discontinuity by using a windowless photomultiplier. Efforts to improve the Lyman discontinuity measurements will continue.

8-4.3.2.1 PLASMA BEHAVIOR IN PHOENIX. Lorentz force interactions are observed to vary with time as the magnetic field increases or decreases on a hydrogen plasma at, e.g., 6×10^{6} cm^{-3}, 10^{-6} mm Hg, ~25 K gauss and with a confinement of τ = 1 msec. As the pressure decreases, density increases and a spike of instability occurs. These density bursts occur as a result of (a) gas puffs and (b) a drop in neutral emissions. Neutral emission can be correlated to ion density and hence measures fluctuation in the number density of ionized hydrogen. It is believed that this fluctuation can be correlated to the energy state which is ionized as the magnetic field increases or decreases past the state. For example, the ionization state n = 12 is observed in the plasma fringe and n = 10 is observed in the center for a 50 K gauss field.

8-5.1 EXPERIMENTAL DEVICES AND RESEARCH AT CENTRE d ETUDES NUCLÉAIRES FONTENAY-AUX-ROSES.

8-5.3 DECA II. Deuterium plasma injected from an electrodeless gun into this mirror machine moves in a 4 meter long drift space with a 10 to 1 static magnetic field increase. Density measurements were made with Faraday cups and 4 and 8 mm microwave interferometers. Transverse energy was determined by measuring the ion flux transmitted through an external magnetic barrier and by magnetic probe. With an optimum magnetic field of ~1.5 K gauss ion density was $2.5 \times 10^{13}/cm^{3}$, transverse energy was 340 ev and mean velocity was 3.9×10^{7} cm/sec. The average plasma pitch angle was a fairly constant 30° over the entire plasma puff.

DISTRIBUTION

Director of Defense, Research and Engineering, Washington 25, D. C..... 1 copy
Assistant to the Secretary of Defense (Atomic Energy), Washington 25, D. C..... 1 copy
Director, Division of Military Application, U.S. Atomic Energy Commission, 1901 Constitution Ave., N.W., Washington 25, D. C..... 2 copies
Chairman, Joint Advanced Study Group, Joint Chiefs of Staff, Washington 25, D. C..... 1 copy
Manager, Albuquerque Operations Office, U.S. Atomic Energy Commission, P. O. Box 5400, Albuquerque, New Mexico..... 1 copy
Manager, U.S. Atomic Energy Commission, San Francisco Operations Office, 2111 Bancroft Way, Berkeley 4, California..... 1 copy
Joint Strategic Plans Group (Rainbow Team), Washington 25, D. C..... 1 copy
Director, Weapons Systems Evaluation Group, Office of the Secretary of Defense, Washington 25, D. C..... 1 copy
Dr. Herbert Scoville, Jr., Assistant Director, Central Intelligence Agency, Washington 25, D. C..... 1 copy
Chief, Defense Atomic Support Agency, Washington 25, D. C..... 5 copies
Vice President, Sandia Corporation, ATTN: E. A. Paxton, Tech Library, P. O. Box 969, Livermore, California..... 1 copy
President, Sandia Corporation, ATTN: Dr. G. C. Dacey, Sandia Base, Albuquerque, New Mexico..... 1 copy
Director, Lawrence Radiation Laboratory, ATTN: Dr. C. M. Van Atta, P.O. Box 808, Livermore, California..... 1 copy
Oak Ridge National Laboratory, ATTN: Dr. E. D. Shipley, Oak Ridge, Tennessee.... 1 copy
Director, Los Alamos Scientific Laboratory, Los Alamos, New Mexico..... 1 copy
Princeton Plasma Physics Laboratory, ATTN: Dr. E. C. Tanner, Princeton, New Jersey..... 1 copy
Massachusetts Institute of Technology, Plasma Dynamics Committee, ATTN: Dr. D. J. Rose, Cambridge, Massachusetts..... 1 copy
Commanding Officer, Los Angeles Ordnance District, ATTN: Dr. Humbert Morris, 55 South Grand Ave., Pasadena, California..... 1 copy
U,S. Atomic Energy Commission, Reference Branch, Technical Information Service Extension, P. O. Box 62, Oak Ridge, Tennessee..... 3 copies
University of California, Lawrence Radiation Laboratory, ATTN: Mr. William R. Baker, Building 52, Berkeley, California..... 1 copy

Department of the Army

Chief of Engineers, Department of the Army, ATTN: ENGRD-SE, Washington 25, D.C. 1 copy
Chief of Research and Development, Department of the Army, Washington 25, D. C.... 1 copy
Commanding General, U.S. Army Materiel Command, Department of the Army, Washington 25, D. C..... 1 copy
Director, Office of Special Weapons Development, Fort Bliss 16, Texas..... 1 copy
Commanding Officer, Picatinny Arsenal, ATTN: ORDBB-TK, Dover, New Jersey..... 1 copy
Commanding General, Aberdeen Proving Ground, ATTN: Ballistics Research Laboratory, Aberdeen, Maryland..... 1 copy
Commanding General, U.S. Army Munitions Command, Picatinny Arsenal, Dover, New Jersey..... 1 copy

Commanding Officer, U.S. Army Research Office (Durham), ATTN: Dr. Hermann Robl, Box CM, Duke Station, Durham, North Carolina ..... 1 copy
Commanding General, Army Rocket and Guided Missile Agency, ATTN: Mr. James Norman, Redstone Arsenal, Alabama ..... 1 copy
Commanding Officer, Diamond Ordnance Fuze Laboratories, ATTN: Mr. Fred Harris, Washington 25, D. C. ..... 1 copy

Department of the Navy

Chief of Naval Operations, Department of the Navy, ATTN: OP-36, Washington 25, D. C. ..... 1 copy
Chief of Naval Operations, Department of the Navy, ATTN: OP-604, Washington, 25, D. C. ..... 1 copy
Chief of Naval Research, Department of the Navy, Washington 25, D. C. ..... 1 copy
Commandant of the Marine Corps, ATTN: Code A03H, Washington 25, D. C. ..... 1 copy
Special Projects Office, Department of the Navy, ATTN: Dr. John Carver, Washington 25, D. C. ..... 1 copy
Chief, Bureau of Naval Weapons, Department of the Navy, Washington 25, D. C. ..... 1 copy
Commander, U.S. Naval Ordnance Laboratory, White Oak, Silver Spring, Maryland .. 1 copy
Director, U.S. Naval Research Laboratory, ATTN: Mrs. Katherine H. Cass, Washington 25, D. C. ..... 1 copy
Commander, U.S. Naval Ordnance Test Station, China Lake, Inyokern, California .... 1 copy
Commanding Officer and Director, U.S. Naval Radiological Defense Laboratory, San Francisco 24, California ..... 1 copy

Department of the Air Force

Deputy Chief of Staff, Development, Department of the Air Force, Washington 25, D.C. 1 copy
Office for Atomic Energy, Department of the Air Force, Building T, 14th &Constitution Ave., Washington 25, D. C. ..... 1 copy
Deputy Chief of Staff, Development, Department of the Air Force, ATTN: AFDDC, Washington 25, D. C. ..... 1 copy
Headquarters, USAF, ATTN: AFTAC, Washington 25, D. C. ..... 1 copy
Commander, Air Force Special Weapons Center, Kirtland Air Force Base, Albuquerque, New Mexico ..... 1 copy
Commander, Air Force Systems Command, Andrews Air Force Base, Washington 25, D. C. ..... 1 copy
Assistant for Operations Analysis, Department of the Air Force, Washington 25, D.C. 1 copy